Int J Clin Exp Med 2012;5(2):201-207
www.ijcem.com /ISSN:1940-5901/IJCEM1202007

Case Report

Imaging astrocytosis with PET in Creutzfeldt-Jakob disease: case report with histopathological findings

Henry Engler[1,2,3,7], Inger Nennesmo[4], Eva Kumlien[5], Juan Pablo Gambini[2], PO Lundberg[5], Irina Savitcheva[5], Bengt Långström[6]

[1]Department of Nuclear Medicine, Uppsala University Hospital, Sweden; [2]Department of Nuclear Medicine, University Hospital of Clinics, Montevideo, Uruguay; [3]Center of Nuclear Research, Faculty of Sciences, Montevideo, Uruguay; [4]Department of Pathology, Karolinska University Hospital, Huddinge, Stockholm; [5]Department of Radiology, Karolinska University Hospital, Huddinge, Stockholm; [6]Department of Organic Chemistry, Uppsala University, Sweden; [7]Centro Uruguayo de Imagenología Molecular, CUDIM, Uruguay

Received February 17, 2012; accepted March 29, 2012; Epub April 6, 2012; Published April 30, 2012

Abstract: In a previous study, patients with suspect Creutzfeldt-Jakob's disease (CJD) have been examined with Positron Emission Tomography (PET) combining *N*-[11C-methyl]-L-deuterodeprenyl (DED) and [^{18}F] 2-fluorodeoxyglucose (FDG) in an attempt to detect astrocytosis and neuronal dysfunction, two of the hallmarks in CJD. Increased DED uptake with pronounced hypometabolism matching the areas with high DED retention was found in the fronto-parieto-occipital areas and cerebellum of patients with confirmed CJD. However, the temporal lobes did not present such a pattern. In 6 of the 15 examined patients the autopsy was performed, but a strict comparison between the PET results and the histopathology could not be done. Recently, one patient with suspect CJD was examined with PET using DED and FDG. The results of the examinations in this patient showed a pattern similar to that found in the brain of the CJD patients from the first study. The patient died shortly after the examination and an autopsy could be performed. The autopsy showed neuronal death, astrocytosis and spongiform changes in the brain. The diagnosis of definite sporadic CJD was established by the Western blot analysis, confirming the presence of the prion resistant protein (PrPres). The PET data demonstrated high DED uptake and extreme low glucose uptake in the left brain hemisphere whereas the right side was less affected. The autopsy was performed allowing the comparison between high DED uptake and the histopathological findings of reactive astrocytosis revealed by immunostaining with antibodies against glial fibrillary acid protein (GFAP). The results confirmed the presence of a pattern with high ratio DED/FDG, similar to that found in the previous study and revealing for the first time, a good correlation between high DED uptake and high density of reactive astrocytes as demonstrated by immunostaining.

Keywords: Astrocytosis, PET, CJD, histopathology

Introduction

The use of DED, an irreversible Mono-amino-oxidase B (MAO-B) inhibitor, has been shown to be useful as a marker of astrocytosis/gliosis [1-6] whereas changes in glucose metabolism measured by the uptake of FDG have been utilized as a marker of neuronal dysfunction to detect hypo- or hypermetabolic changes [7-8]. In the first PET study performed in patients with suspect CJD using DED (to reveal *in vivo* reactive astrocytosis) and FDG (to detect signs of neuronal death) we reported that the combination of these tracers could reveal a pattern of diagnostic value [9].

A patient with rapid onset dementia, ataxia and myoclonus was examined at Uppsala PET Centre, Sweden, and the combination of tracers DED and FDG was selected with the intention of detecting the presence of astrocytosis and neuronal dysfunction.

Shortly after the examination the patient died and an autopsy was performed to compare the correlations between histopathological and PET findings.

Subject and methods

The patient

The patient was a 64-year-old man with heredity for cardiovascular disease. He had a history of

hypertension, myocardial infarction and atrial fibrillations. He was a non smoker having a history of alcohol abuse. After a suspected virus infection, he complained about dizziness and memory problems. Two weeks later his behaviour was repetitive and he could no longer follow a television program. One week later he was incapable of writing his name, became disorientated and had visual hallucinations. Speech difficulties were present and he was unable to follow simple instructions. He had severe ataxia but muscle tone and tendon reflexes were normal. Myoclonic jerks were observed in the right arm. Cerebrospinal fluid was normal concerning cells and proteins. Analysis of protein 14-3-3 was not available at the laboratory. Complete blood count was normal but liver probes were slightly increased. Magnet resonance tomography (MRI) of the brain was unremarkable. Repeated EEG investigations were characterized by bilateral symmetric trifasic waves with frequency 1 Hz with slow background activity of delta type 2-2, 8 Hz. The condition rapidly deteriorated and five weeks after the disease onset, the patient died.

Radiotracers

Production of FDG and DED was done according to the standard good manufacturing practice (GMP) at Uppsala Imanet. Synthesis of ^{11}C-L-deprenyl was prepared as described previously [10-12].

PET-scanning

The scans were performed using a Siemens ECAT EXACT HR+ scan, (CTI PET-systems Inc.) with an axial field of view of 155 mm, providing 63 contiguous 2.46 mm slices with a 5.6 mm transaxial and a 5.4 mm axial resolution. The patient was scanned after fasting for 4 hours. The orbito-meatal line was used to center the head of the subjects. The tracer doses were given intravenously and the data were acquired in 3-D mode. For FDG, the injected dose was 432 MBq. PET measured the radioactivity in the brain for 2x60, 2x180, 2x300, and 1x600 seconds frame during 45 minutes.

The tracer dosis for DED was 430 MBq. PET measured the radioactivity in the brain for 4x30, 2x60, 1x300, and 5x600 seconds frames for 59 minutes. Attenuation correction was based on a 10-minute windowed transmission scan with rotating 68Ge rod sources before administration of the radioactivity. The emission data were normalized, corrected for random coincidences and dead time, and corrected for scatter using a method by Watson and colleagues [13]. Images were reconstructed with the standard software supplied with the scanner (ECAT 7.1; CTI PET Systems, Knoxville, TN), using Fourier rebinning followed by two-dimensional filtered back-projection applying a 4mm Hanning filter.

Both scans were performed the same day. The DED examination was performed first and the FDG administration, two hours after the start of the DED scan.

Propofol anaesthesia was applied according to previous experience [9] in patients with suspected CJD.

Regions of Interest (ROI)

The set of ROI applied was the same as used in other studies and has been described in detail before [9, 14-17]. The following areas were included in the analyses: frontal, parietal, temporal, occipital and cerebellar cortices, pons, white matter and striatum.

A computerized re-orientation procedure was used to align the two PET studies for accurate comparisons [18]. The DED images were realigned to the FDG acquisition images.

Tracers

DED: Quantitative estimates on binding to MAO-B as well as initial tracer distribution were generated by the Patlak method [19], with proposed modifications [12] following the same procedure as in a previous study [9]. The tracer uptake on a pixel-by-pixel basis was divided by the cerebellar cortex tracer concentration and plotted against normalized time, although the cerebellar time activity data were first multiplied by an exponential. The procedure has been shown to linearize the Patlak graph slope and allows a separate generation of images representing the Patlak slope and intercept. This slope is also found proportional to MAO-B enzyme expression [12].

FDG: Parametric maps of glucose metabolic rate were generated by the Patlak-technique. Images of glucose metabolic rate (CMRglu) were

generated with an operational equation derived by Sokoloff [13] and modified by Phelps [14].

Statistical analysis of PET data

The values for glucose metabolic rate and binding of DED obtained in patients were compared with those in healthy volunteers, and deviations larger than ±2SD were considered significant. The values of glucose metabolic rate were normalized to the whole brain to calculate a glucose metabolic index. For DED, the absolute Patlak slope values in patients were compared directly with those in the healthy subjects [9].

Pathology

Brain samples were collected for molecular genetic analysis before the brain was prepared for examination. After seven weeks of fixation in 4% formaldehyde the brain was cut in coronal sections for routine diagnostic histopathology. Several cortical areas from the different lobes, hippocampus, basal ganglia, thalamus, mesencephalon, brainstem and cerebellum were included. Furthermore, ten different regions of the brain, cortex, cerebellum and basal ganglia, were studied following the results of the PET-DED study where high binding was observed. Some of the contralateral areas with low DED binding were also studied. The thalami showed low DED activity but were included as well. The tissue was treated with formic acid for one hour before paraffin embedding. The sections were stained with haematoxylin-eosin, Luxol fast blue and Bielschowsky's silver stain. Immunostaining with antibodies against glial fibrillary acid protein (GFAP) was also performed.

A piece of frozen brain tissue was examined at the National CJD Surveillance Unit (University of Edinburgh, Western General Hospital) to detect the presence of protease resistant PrP.

Results

PET findings

FDG: The CMRglu in the whole brain was estimated to 19 micromole/min/100g, which is 53% lower than normal. The uptake in the cerebellum and pons were decreased approximately 40%. All regions in the brain showed 10-68% decreased glucose uptake. Changes were less pronounced in temporal lobes (11-60%) and more pronounced in the parietal cortex (54-64%). In basal ganglia 56-62% decrease was measured and in thalami 54-68% (right and left). Lower FDG uptake was observed in the left hemisphere compared with the right in lateral parts of the frontal cortex (11-16%), in extensive areas of the parietal cortex (13-17%) and 8-26% in the temporal cortex.

DED: Slope values for DED revealed bilaterally, 33-39% higher binding than expected, in cerebellum. DED values were increased most in the left side. In frontal association cortex the binding in the left side was increased 16%, in most of the parietal cortex 12-24%, in the basal ganglia 11% and in the temporal lobe 10-18%, affecting the antero-inferior and postero-lateral regions. In the right side, the only region with enhanced DED binding was the medial anterior part of the temporal lobe (13). DED binding was normal in the thalamic nuclei. In the left hemisphere, the DED binding was higher than in the right hemisphere in the frontal associative cortex (10%), parietal cortex (16-30%), and in the lateral region of the temporal lobe (13%-18%). The pattern previously described (low FDG and high DED) was found in the frontal and parietal cortices of the left hemisphere. In this patient these changes were also found in the lateral part of the left temporal lobe (**Figure 1**). The right hemisphere did not present the same high ratio DED/FDG (**Figure 2**). To compare the results with the previous study [9], values in Standard Deviations (SD) were analysed. Values over 2 SD were considered significants for the DED binding and under 2 SD for FDG uptake, which means more than10% difference compared with controls. The left hemisphere reveals the same pattern of uptake with high ratio DED/FDG fronto-parietal described previously [9]. Occipital cortex in this patient did not present high DED/FDG ratio. Like in the previous study [9] relative high metabolism was found in temporal lobes compared with the whole brain, caused by the extremely low uptake in the rest of the brain.

Pathological findings

Microscopical examination of different cortex cerebri regions showed widespread loss of neurons, increased number of glial cells and spongiform changes affecting the whole thickness of the cortex. Similar changes were found in putamina and caudate nuclei. Only very discrete

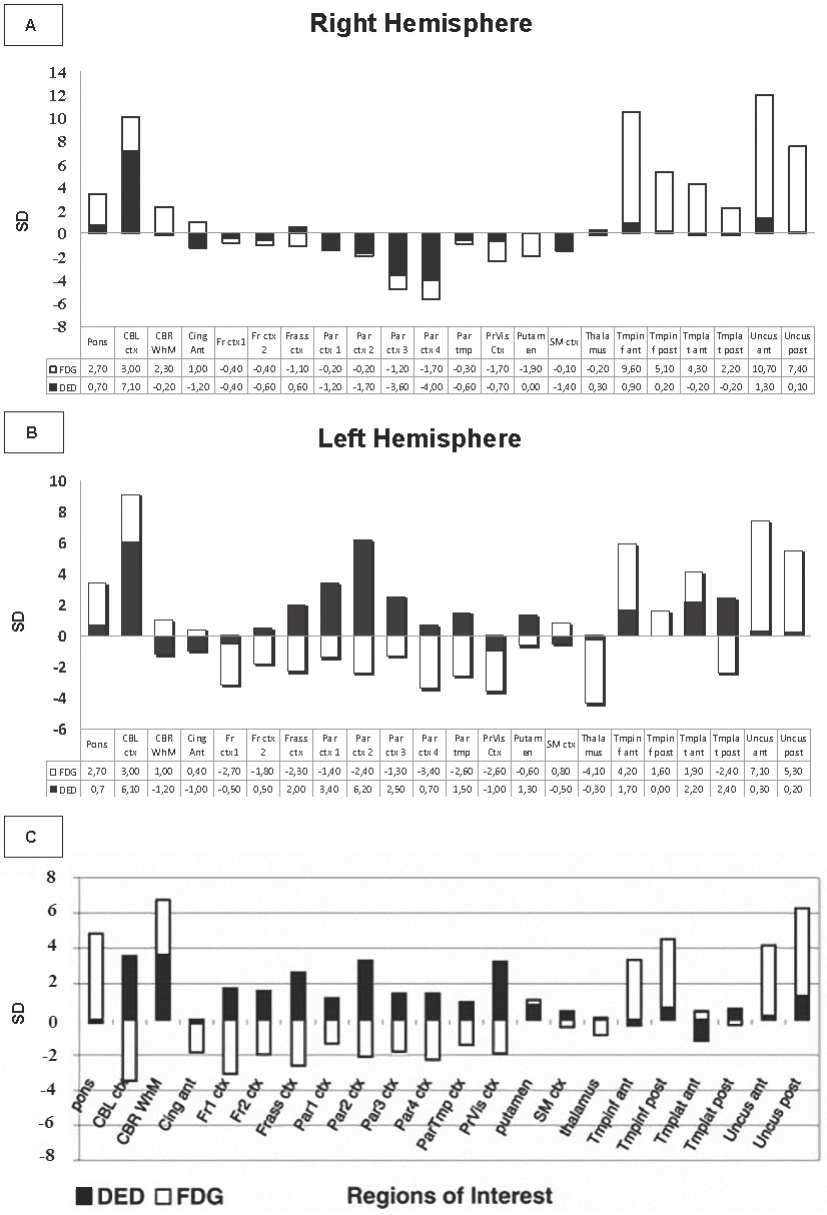

	Pons	CBL ctx	CBR WhM	Cing Ant	Fr ctx1	Fr ctx 2	Frass ctx	Par ctx 1	Par ctx 2	Par ctx 3	Par ctx 4	Par tmp	PrVis Ctx	Putamen	SM ctx	Thalamus	Tmpinf ant	Tmpinf post	Tmplat ant	Tmplat post	Uncus ant	Uncus post
FDG	2,70	3,00	2,30	1,00	-0,40	-0,40	-1,10	-0,20	-0,20	-1,20	-1,70	-0,30	-1,70	-1,90	-0,10	-0,20	9,60	5,10	4,30	2,20	10,70	7,40
DED	0,70	7,10	-0,20	-1,20	-0,40	-0,60	0,60	-1,20	-1,70	-3,60	-4,00	-0,60	-0,70	0,00	-1,40	0,30	0,90	0,20	-0,20	-0,20	1,30	0,10

	Pons	CBL ctx	CBR WhM	Cing Ant	Fr ctx1	Fr ctx 2	Frass ctx	Par ctx 1	Par ctx 2	Par ctx 3	Par ctx 4	Par tmp	PrVis Ctx	Putamen	SM ctx	Thalamus	Tmpinf ant	Tmpinf post	Tmplat ant	Tmplat post	Uncus ant	Uncus post
FDG	2,70	3,00	1,00	0,40	-2,70	-1,80	-2,30	-1,40	-2,40	-1,30	-3,40	-2,60	-2,60	-0,60	0,80	-4,10	4,20	1,60	1,90	-2,40	7,10	5,30
DED	0,7	6,10	-1,20	-1,00	-0,50	0,50	2,00	3,40	6,20	2,50	0,70	1,50	-1,00	1,30	-0,50	-0,30	1,70	0,00	2,20	2,40	0,30	0,20

Figure 1. A, BA: Right hemisphere. B: Left hemisphere: Stacked bar graphs showing the mean FDG and DED change from normal (in standard deviations) for each ROI in the patient with CJD in the right and left hemispheres. FDG values are normalized to the whole brain for FDG. Standard Deviations of expected slope values were used. C: Bar graph showing the DED/FDG ratio in the mentioned areas in patients with CJD [9]. Ant, anterior; inf, inferior; post, posterior; ctx, cortex; CBL, cerebellum; CBR WhM, cerebral white matter; Cing, cingulum; Fr, frontal 1-2: basal to apical; Frass, frontal association ctx; Par, parietal(1-4: basal to apical); ParTmp, parietotemporal; PrVis, primary visual ctx; SM, sensorimotor ctx; Th, thalamus; tmp, temporal ctx.

spongiform degeneration was detected in the thalami. The mesencephalon and brainstem did not reveal pathological changes. Spongiform changes, gliosis and loss of Purkinje cells were seen in the molecular layer of the cerebellar cortex.

GFAP immunostaning

The immunoreactivity for GFAP in the cerebral cortex was more pronounced in the left hemisphere than in the right.

The number of immunopositive astrocytes varied within the cortex. Often they were present in the whole thickness of the cortex. In sections from the right hemisphere the immunoreactivity was usually restricted to the most superficial layer but sometimes also deeper layers of the cortex were involved.

The number of astrocytes was higher in the basal ganglia on the left than on the right side. No obvious difference was found between the two thalamic nuclei.

In sections from the cerebellar hemispheres a strong immunoreactivity was present on both sides, especially in the molecular layer and especially in regions with many GFAP-positive as-

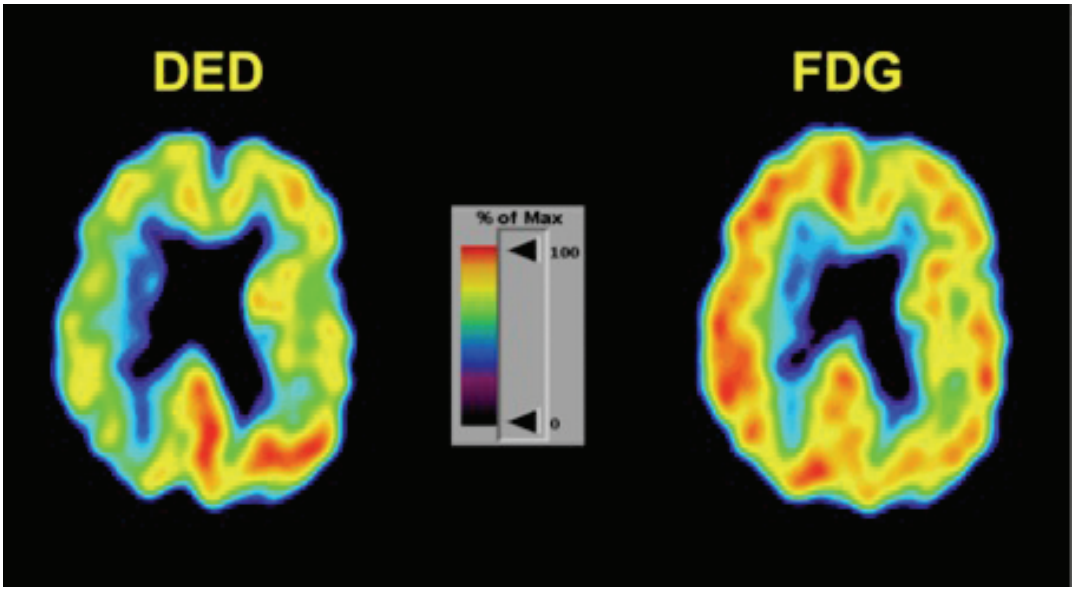

Figure 2. DED and FDG show a typical pattern with increased DED binding (astrocytosis) and decreased glucose metabolism (cell dysfunction).

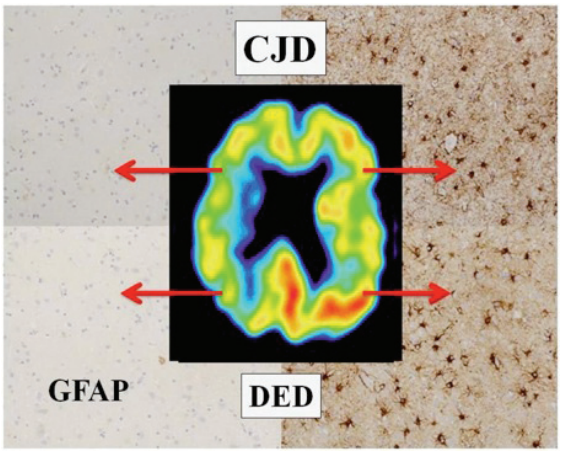

Figure 3. PET indicates increased DED binding in the left hemisphere. Histopathology of the frontal and parietal cortices shows GFAP-positive astrocytes in the sites with high DED binding.

trocytes in the granular cell layer below (**Figure 3**).

Molecular genetic analysis

The Western blot analysis confirmed the presence of protease-resistant PrP with a Type 1 isotype, characteristic of sporadic CJD. The patient was methionine homozygote at codon 129 with no pathogenic mutations or insertions in the prion gene.

Discussion

The diagnosis of definite CJD is at present only possible through neuropathological examination of brain tissue according to international (WHO and EU) consensus and the demonstration of the presence of the PrPres. For ethical, practical and topographic reasons, brain biopsy is not applicable. Computed tomography (CT) scans show only unspecific changes whereas magnetic resonance imaging (MRI) may be of help but is often inconclusive. Periodic sharp wave complexes are found as typical EEG changes in certain genotypes. Laboratory examinations of cerebrospinal fluid for proteins such as 14.3.3 and tau are of importance in the diagnosis of certain types of CJD, e.g. sporadic versus variant type CJD, but may be normal, even in pathologically confirmed cases. So far, no blood assay is available that may help in the diagnosis. There is thus a need for a technique that can illuminate the neuropathological changes in the living patient [9].

In our first study we found that the regional distribution of the DED/FDG changes was clearly asymmetrical left to right in eight of the patients

[9]. There was also an uneven distribution as regarding the DED/FDG changes in different areas of the cerebral cortex and the cerebellum. However, in the first study we had difficulties to compare in detail particular regions of interest obtained with PET with the samples of cerebral cortex usually investigated by the neuropathologists. It was also difficult to compare the DED/FDG findings with the clinical picture with one exception: in a patient with the Heidenhain subtype of sporadic CJD [9]. In this patient very strong correlations were found between the clinical symptoms and signs of cortical blindness and visual hallucinations, and the neuropathological changes in the occipital cortex characterized by very high DED uptake (>11 SD) in both sides in the occipital cortex. This is the first time we could perform a careful selection of the regions we wanted to examine histopathologically for comparison with the PET results. We found a strong correlation between regions with increased DED binding and prominent gliosis.

Conclusions

The use of PET and a tracer combination including FDG and DED seems to be an excellent tool to detect neurodegenerative changes in vivo characterized by neuronal dysfunction and reactive astrocytosis. The pattern of high ratio DED/FDG found in patients with CJD could for first time be investigated in an autopsy according to the results of the PET DED examination, the PET data, revealing a clear correlation between the the astrocytosis detected with the GFAP and the increased DED binding.

Address correspondence to: Dr. Henry Engler, Uruguayan Centre of Molecular Imaging (CUDIM), Montevideo, Uruguay, Department of Nuclear Medicine, University Hospital of Clinics, Montevideo, Uruguay, Center of Nuclear Research, Faculty of Sciences, Montevideo, Uruguay, Department of Nuclear Medicine, Uppsala University Hospital, Sweden E-mail: Henry.Engler@cudim.org

References

[1] Ekblom J, Aquilonius SM, Jossan SS. Differential increases in catecholamine metabolizing enzymes in amyotrophic lateral sclerosis. Exp Neurol 1993; 123: 289-294.

[2] Fowler JS, MacGregor RR, Wolf AP, Arnett CD, Dewey SL, Schlyer D, Christman D, Logan J, Smith M, Sachs H, Aquilonius SM, Bjurling P, Halldin C, Hartyig P, Leenders KL, Lundqvist H, Oreland L, Stalnacke C-G, Langstrom B. Mapping human brain monoamine oxidase A and B with 11C-labeled suicide inactivators and PET. Science 1987; 235: 481-485.

[3] Jossan SS, d'Argy R, Gillberg PG, Aquilonius SM, Langstrom B, Halldin C, Bjurling P, Stålnacke C-G, Fowler J, MacGregor R, Oreland L. Localization of monoamine oxidase B in human brain by autoradiographical use of 11C-labelled L-deprenyl. J Neural Transm 1989; 77: 55-64.

[4] Jossan SS, Gillberg PG, d'Argy R, Aquilonius SM, Langstrom B, Halldin C, Oreland L. Quantitative localization of human brain monoamine oxidase B by large section autoradiography using L-[3H] deprenyl. Brain Res 1991; 547: 69-76.

[5] Nakamura S, Kawamata T, Akiguchi I, Kameyama M, Nakamura N, Kimura H. Expression of monoamine oxidase B activity in astrocytes of senile plaques. Acta Neuropathol 1990; 80: 419-425.

[6] Stenstrom A, Arai Y, Oreland L. Intra- and extraneuronal monoamineoxidase-A and -B activities after central axotomy (hemisection) on rats. J Neural Transm 1985; 61: 105-113.

[7] Alavi A, Dann R, Chawluk J, Alavi J, Kushner M, Reivich M. Positron emission tomography imaging of regional cerebral glucose metabolism. Semin Nucl Med 1986; 16: 2-34.

[8] Handforth A, Cheng JT, Mandelkern MA, Treiman DM. Markedly increased mesiotemporal lobe metabolism in a case with PLEDs: further evidence that PLEDs are a manifestation of partial status epilepticus. Epilepsia 1994; 35: 876-881.

[9] Engler H, Lundberg PO, Ekbom K, Nennesmo I, Nilsson A, Bergstrom M, Tsukada H, Hartvig P, Långström B. Multitracer study with positron emission tomography in Creutzfeldt-Jakob disease. Eur J Nucl Med Mol Imaging 2003; 30: 85-95.

[10] Fowler JS, Wolf AP, MacGregor RR, Dewey SL, Logan J, Schlyer DJ, Langstrom B. Mechanistic positron emission tomography studies: demonstration of deuterium isotope effect in the monoamine oxidase-catalyzed binding of [11C]L-deprenyl in living baboon brain. J Neurochem 1988; 51: 1524-1534.

[11] MacGregor RR, Fowler JS, Wolf AP, Halldin C, Langström B. Synthesis of suicide inhibitors of monoamine oxidase: carbon-11 labeled clorgyline, L-deprenyl and D-deprenyl. J Labelled Comp Radiopharm 1988; 25: 1-9.

[12] Bergström M, Kumlien E, Lilja A, Tyrefors N, Westerberg G, Långström B. Temporal lobe epilepsy visualized with PET with 11C-L-deuterium-deprenyl-analysis of kinetic data. Acta Neurol Scand 1998; 98: 224-231.

[13] Sokoloff L, Reivich M, Kennedy C, Des Rosiers MH, Patlak CS, Pettigrew KD, Sakurada O, Shinohara M. The [14C]deoxyglucose method for the measurement of local cerebral glucose utilization: theory, procedure, and normal values in the conscious and anesthetized albino rat. J Neuro-

chem 1977; 28: 897-916.
[14] Phelps ME, Huang SC, Hoffman EJ, Selin C, Sokoloff L, Kuhl DE. Tomographic measurement of local cerebral glucose metabolic rate in humans with (F-18)2-fluoro-2-deoxy-D-glucose: validation of method. Ann Neurol 1979; 6: 371-388.
[15] Engler H, Santillo AF, Wang SX, Lindau M, Savitcheva I, Nordberg A, Lannfelt L, Långström B, Kilander L. In vivo amyloid imaging with PET in frontotemporal dementia. Eur J Nucl Med Mol Imaging 2008; 35: 100-106.
[16] Forsberg A, Engler H, Almkvist O, Blomquist G, Hagman G, Wall A, Ringheim A, Långström B, Nordberg A. PET imaging of amyloid deposition in patients with mild cognitive impairment. Neurobiol Aging 2008; 29: 1456-1465.
[17] Klunk WE, Engler H, Nordberg A, Wang Y, Blomqvist G, Holt DP, Bergström M, Savitcheva I, Huang GF, Estrada S, Ausén B, Debnath ML, Barletta J, Price JC, Sandell J, Lopresti BJ, Wall A, Koivisto P, Antoni G, Mathis CA, Långström B. Imaging brain amyloid in Alzheimer's disease with Pittsburgh Compound-B. Ann Neurol 2004; 55: 306-319.
[18] Andersson JL, Thurfjell L. Implementation and validation of a fully automatic system for intra- and interindividual registration of PET brain scans. J Comput Assist Tomogr 1997; 21: 136-144.
[19] Patlak CS, Blasberg RG, Fenstermacher JD. Graphical evaluation of blood-to-brain transfer constants from multiple- time uptake data. J Cereb Blood Flow Metab 1983; 3: 1-7.
[20] Sokoloff L, Reivich M, Kennedy C, Des Rosiers MH, Patlak CS, Pettigrew KD, Sakurada O, Shinohara M. The [14C]deoxyglucose method for the measurement of local cerebral glucose utilization: theory, procedure, and normal values in the conscious and anesthetized albino rat. J Neurochem 1977; 28: 897-916.
[21] Phelps ME, Huang SC, Hoffman EJ, Selin C, Sokoloff L, Kuhl DE. Tomographic measurement of local cerebral glucose metabolic rate in humans with (F-18)2-fluoro-2-deoxy-D-glucose: validation of method. Ann Neurol 1979; 6: 371-388.